Laboratory Investigation (2021) 101:808–823
https://doi.org/10.1038/s41374-021-00541-5

ARTICLE

DDAH-1, via regulation of ADMA levels, protects against ischemia-induced blood-brain barrier leakage

Yichen Zhao[1] · Xiaoye Ma[1] · Yuchen Zhou[1] · Junchao Xie[1] · Xueyuan Liu[1] · Yanxin Zhao[1]

Received: 17 October 2020 / Revised: 5 January 2021 / Accepted: 7 January 2021 / Published online: 11 February 2021

Abstract

Dimethylarginine dimethylamino hydrolase-1 (DDAH-1) is an important regulator of nitric oxide (NO) metabolism that has been implicated in the pathogenesis of cardiovascular diseases. Nevertheless, its role in cerebral ischemia still needs to be elucidated. Herein, we examined the expression of DDAH-1 in the brain of rat by double-label immunofluorescence staining. DDAH-1 knock-out (DDAH-$1^{-/-}$) and wild-type rats underwent middle cerebral artery occlusion/reperfusion (MCAO/R). After 24 h, neurological scores, TTC staining and TUNEL assay were used to evaluate neurological damages. 3 and 7-days infarct outcomes were also shown. Blood-brain-barrier (BBB) permeability was examined via Evans blue extravasation and tight junction (TJ) proteins expression and mRNA levels by western blot and RT-qPCR. The levels of plasma asymmetric dimethylarginine (ADMA), NO and ADMA in brain tissue were also assessed. In addition, supplementation of L-arginine to DDAH-$1^{-/-}$ rats was used to explore its role in regulating NO. DDAH-1 was abundantly distributed in cerebral cortex and basal nuclei, and mainly expressed in neurons and endothelial cells. DDAH-$1^{-/-}$ rats showed aggravated neurological damage and BBB disruption, including decrease of TJ proteins expression but indistinguishable mRNA levels after MCAO/R. DDAH-1 depletion and neurological damages were accompanied with increased ADMA levels and decreased NO concentrations. The supplementation with L-arginine partly restored the neurological damages and BBB disruption. To sum up, DDAH-1 revealed to have a protective role in ischemia stroke (IS) and IS-induced leakage of BBB via decreasing ADMA level and possibly via preventing TJ proteins degradation.

Introduction

Stroke is the leading cause of death and the major cause of disability, with ischemia stroke (IS) accounting for as much as 80% of these cases [1, 2]. IS is characterized by endothelial dysfunction, which mainly depends on the production of nitric oxide (NO). NO is synthesized from L-arginine by a family of NO synthases (NOS), that target soluble guanylyl cyclase thus having a critical role in various signaling pathways, and especially in regulation of vascular function. NO in physiological concentrations is beneficial to vasodilatation and integrity of vascular structure [3–6], and its production could be inhibited by asymmetric dimethylarginine (ADMA), due to its structure that is competitive with NOS. ADMA is derived from methylated arginine residues found on proteins by a group of protein-arginine methyl transferase's and is largely eliminated by dimethylarginine dimethylamino hydrolase (DDAH). Therefore, DDAH is thought to regulate the production of endothelial NO through DDAH-ADMA-NOS axis. There are two isoforms of DDAH, DDAH-1 and DDAH-2; DDAH-1 seems to have greater effects on ADMA-dependent NO production [7–9].

ADMA has been identified as cardiovascular risk factor for various clinical conditions [10–18]. DDAH-1 dysfunction has also been linked with pulmonary hypertension, coronary heart disease, hypertension, congestive heart failure, portal hypertension and many other diseases [19–27]. Nonetheless, so far only few studies have addressed the role

Supplementary information The online version contains supplementary material available at https://doi.org/10.1038/s41374-021-00541-5.

✉ Xueyuan Liu
shsylxy@126.com

✉ Yanxin Zhao
zhao_yanxin@126.com

[1] Department of Neurology, Shanghai Tenth People's Hospital, Tongji University School of Medicine, No.301 Middle Yanchang Road, Shanghai 200072, PR China

of DDAH-1 in IS. Leypoldt et al. have suggested that overexpression of DDAH-1 cannot protect from ischemic cerebral tissue damage, since high basal cerebral DDAH activity could not be furthermore increased by overexpression of DDAH-1 [28].

Here, by using a novel DDAH-1 knockout rat strain, we studied the effect of DDAH-1 dysfunction on IS in rats. The rat middle cerebral artery occlusion/reperfusion (MCAO/R) model was used to mimic IS pathogenesis in human. Neurological scores, TTC staining, TUNEL assay and blood-brain-barrier (BBB) leakage assessment of 24-h were used to evaluate acute neurological damages, and long-term outcomes of 3 and 7-days were also shown by neurological scores and TTC staining. L-arginine, as a substrate of NO synthesis, was supplemented and combined with ADMA level assessment to ensure the relationship between DDAH-1 and NO. The aim of the present study was to explore the role of DDAH-1 in IS, which we hypothesized would act as a protective factor for IS, and investigate the possible pathways.

Materials and methods

Animals

DDAH-1 knockout (KO) (DDAH-$1^{-/-}$) Sprague–Dawley (SD) rats were kindly provided by Professor Da-Chun Xu (Department of Cardiology, Shanghai Tenth People's Hospital, Tongji University School of Medicine). The generation of DDAH-$1^{-/-}$ rats were the same as previously described [29]. The CRISPR-Cas9 technique was applied to generate DDAH-$1^{-/-}$ rats on SD background as illustrated in Fig. S1. Wild-type (WT) male SD rats, weighing 250 g to 280 g (8–10 weeks of age) were purchased from Shanghai SIPPR-BK laboratory animal Co. Ltd. All rats were housed in separated cages in SPF animal room at 25 °C and humidity of 40% with a 12-h light/dark cycle, and were given free access to water and diet. In addition, all animal studies (including the rats euthanasia procedure) were conducted according to the U.K. Animals (Scientific Procedures) Act, 1986 and associated guidelines. L-Arginine (2.0% L-Arginine (ARG) in drinking water) was used as indirect supplement of DDAH-1. A randomized ARG and vehicle feeding schedule was created using the standard = RAND () function in Microsoft-Excel and prepared by a third person not involved in the experiment to maintain blinding.

Genotyping

The KO SD rats were generated by pantogamy. To identify homozygous (DDAH-$1^{-/-}$) or heterozygous (DDAH-$1^{+/-}$) rats, the DNA sequences (extracted from the tail) were examined in all newborns. DNA Isolation Kit (Sangon Biotech (Shanghai) Co.) was used to extract genomic DNA. The following primers: forward primer, 5′-CATTC ATCCGCTGCCAAGAG-3′; reverse primer, 5′-CTGGC CCTTTACCTCCTTCC (Shanghai JIE LI Biology Co.) were used for PCR amplification. The PCR products were purified by agarose gel electrophoresis. Finally, only homozygous DDAH-$1^{-/-}$ rats were selected for further experiments. DNA electrophoresis for KO and WT rats was shown in supplementary material (Fig. S2).

MCAO/R model

All animals were fasted but had free access to water 12 h before the experiment. Each rat was weighed before surgery and anesthetized intraperitoneally with 2% pentobarbital sodium (0.2 ml/100 g) (0.3 mL/100 g). Rectal temperature was maintained from 36.5 °C to 37.5 °C by a heating pad. In WT group, KO group and ARG group, rats were subjected to MCAO/R as previously described with some modifications to reduce adverse events [30]. Briefly, following a midline incision, neck vessels including the left common carotid artery, external carotid artery (ECA), and internal carotid artery (ICA) were exposed and isolated. Then, a small incision was made on the ECA and silica suture (Doccol Co.403756PK5Re) and was gently advanced into the ICA for distance of 18–20 mm to occlude the origin of middle cerebral artery. The suture was removed carefully to restore perfusion 90 min later. The neck incision was closed, and rats were allowed access to food and water. In SHAM group, rats underwent the same procedure without inserting the suture. A laser-Doppler probe implanted on the skull (2 mm posterior and 5 mm lateral to the bregma) was to monitor the cerebral blood flow (CBF). Readings were recorded 15 min before operation and after occlusion and reperfusion, and data were expressed as the percentage of baseline value in WT/SHAM group. A floating catheter was inserted into the left femoral artery for monitoring continuous mean arterial blood pressure (MABP). After operation, rats were individually housed and carefully fed until the end of the experiment.

Behavior assessment and TTC staining

The neurobehavioral changes of rats were evaluated by the neurological severity score (NSS) (adapted from [31]). It is consisted of 4 individual parameters including tests on motor function, sensory function, beam balance, reflex absence and abnormal movements, and the total score is 18 points (Table S1).

For measuring infarct volume, TTC staining was performed 24 h, 3 days, 7 days respectively after surgery. Rats were anesthetized and the brain was then collected and

quickly frozen at −20°C for 15 min. Brain tissue was sliced into six coronal sections (2 mm thick) using Leica blades in a rat brain matrix (RWD Life Science Co.). The slices were stained in TTC (Servicebio.Co) for 30 min at 37 °C in the dark followed and fixed with 4% paraformaldehyde (Servicebio.Co). The infarcted tissue was unstained (white), while normal tissue was stained in red. Digital images of brain slices were analyzed using ImageJ software. To avoid possible interference of brain edema, the infarct area on each slice was corrected by standard method (infarct area=contralateral hemisphere area−area of non-ischemic ipsilateral hemisphere). The total infarct area was obtained by addition of infarct area in each section. The infarct volume was calculated by multiplication of the total infarct area with the thickness of each slice. The percentage of infarct volume was also shown as the equation (infarct area/contralateral hemisphere area).

TUNEL assay

Cell apoptosis was analyzed using TUNEL in situ cell death detection kit (Roche, Germany). At 24 h after surgery, rats were deeply anesthetized and then perfused with normal saline and 4% paraformaldehyde. The brain was removed, fixed in 4% paraformaldehyde overnight, and then dehydrated in 30% sucrose solution. The infarct coronal sections in different groups were collected and made into paraffin section (5 μm). Then the apoptotic cells were determined according to the manufacturer's instruction. On the slices, stained dark brown neuron nucleus represented TUNEL-positive, while blue nucleus represented DAPI-positive. The apoptosis rate was expressed as ratio of TUNEL-positive cells to total cells. Using light microscopy (200×), 10 visual fields were randomly selected and approximately 4000 cells were counted in each slice. Finally, the averages of apoptotic number and rate for each group were calculated and compared.

Determination of NO concentration

The NO concentrations in infarct area were observed 24 h after MCAO/R model. Basal ganglia were rapidly isolated and homogenized. After centrifugation of 3000 rpm for 6 min, the supernatant was collected for the determination of NO^{2-}/NO^{3-} contents (μmol/gprotein) according to the manufacturer's instruction of the NO assay kit (Nanjing Jiancheng Bioengineering Institute, China), which indirectly reflected NO concentration.

Determination of ADMA level

The plasma and tissue ADMA concentrations were measured by enzyme-linked immunosorbent assay (ELISA) kit (JianglaiBio, Shanghai, China) following the manufacturer's instruction. Each sample was gauged in triplicate. A standard curve for six standard concentrations and their corresponding OD values (450 nm) was generated to measure the concentration of unknown sample.

Evans blue assessment

Evans blue dye (EBD) extravasation was measured to assess BBB disruption. At 24 h after surgery, 2% EBD in normal saline was injected intravenously (4 mL/kg) via caudal vein and was allowed to circulate. Six h after EBD injection, rats were deeply anesthetized and perfused with normal saline. Subsequently, brains were removed and sliced into six coronal sections (2 mm thick). The whole brains and slices were photographed to analyze the degree of EBD extravasation. For quantitative measurement, the left hemispheres (infarct side) of brain tissue were weighted and homogenized in 250 μL of PBS by ultrasonic processor, after which 250 μL of formamide was added and homogenized. By centrifugation for 5 min at $12000 \times g$, the supernatants of samples were obtained, followed by measuring the absorbance at 610 nm via microplate spectrophotometer. The amount of EBD extravasation was calculated according to a standard curve and the result was expressed as EBD/brain tissue (μg/g).

Western blots

The expression of tight junction (TJ) proteins in brain tissue were analyzed using western blot. At 24 h after surgery, brains were rapidly removed as mentioned above, and tissues around infarct area were collected to extract the whole proteins using the protein extraction kit (Epizyme). Bicinchoninic acid assay was used to determine the concentration of proteins. Equal amount of proteins (50 μg) in different groups were separated by Tris–glycine SDS page (6% and 10%) and transferred to nitrocellulose membrane. Consequently, the membranes were blocked with 5% non-fat milk in PBST at room temperature for 1 h and incubated with primary antibodies (ZO-1,absin, 1:1000; occludin, absin, 1:1000; claudin-5, absin, 1:1000; β-actin, sigma, 1:5000) at 4 °C overnight. The following day, the membranes were incubated with corresponding HRP-conjugated secondary antibody (abcam, 1:2000) at room temperature for 1.5 h. The protein band was scanned on Amersham Imager 600 using enhanced chemiluminescence kit (Sangon Biotech (Shanghai) Co.) and the relative amounts of proteins were analyzed using ImageJ software.

Reverse transcription quantitative polymerase chain reaction (RT-qPCR)

The mRNA level of TJ proteins in infarct area were analyzed using RT-qPCR. The brain tissues of the experimental

Table 1 Primers sequences for GAPDH, ZO-1, occludin, claudin-5 of rat.

Genes	Sequences
ZO-1	F: 5′-CCACCTCGCACGTATCACAAGC-3′
	R: 5′-GGCAATGACACTCCTTCGTCTCTG-3′
occludin	F: 5′-TCGTGATGTGCATCGCTGTATTCG-3′
	R: 5′-CGTAACCGTAGCCGTAACCGTAAC-3′
claudin-5	F: 5′-GCCTCCGCACTGCTCATGTG-3′
	R: 5′-TCTTCTTGTCGTAATCGCCGTTGG-3′
GAPDH	F: 5′-CGTCTTCACCACCATGGAGA-3′
	R: 5′-CGGCCATCACGCCACAGCTT-3′

F forward, *R* reverse, *ZO-1* Zonula Occludens-1, *GAPDH* glyceraldehyde-3-phosphate dehydrogenase, *RT-qPCR* reverse transcription quantitative polymerase chain reaction.

rats were dissected. The tissue (50 mg) around infarct area were extracted and treated with Trizol reagent for the extraction of total RNA, which diluted with ultrapure water. The RNA concentration and purity were estimated using an ultraviolet spectrophotometer (measured by absorbance at 260 nm and 280 nm) and the ratio of OD 260/OD 280 was determined to be between 1.8 and 2.0, which met the needs of the follow-up experiments. The RNA was reversely transcribed into cDNA using PrimeScript RT reagent kit (Takara Bio Inc., Otsu, Japan) and the obtained cDNA was stored at −20 °C. The primers for glyceraldehyde-3-phosphate dehydrogenase (GAPDH), ZO-1, occludin, claudin-5 of rat were designed and synthesized by Shanghai Sangon Biotechnology Co., Ltd. (Shanghai, China) (Table 1). RT-qPCR was conducted with the cDNA according to the instructions of the SYBR FAST qPCR Master Mix (KAPA). The reaction system was 20 μl containing 1 μl of cDNA template SYBR, 10 μl of FAST qPCR Master Mix, 0.4 μl of ROX High, 0.4 μl of Primer F (10 pmol/μl) and Primer R (10 pmol/μl) and 7.8 μl of sterile water. RT-qPCR was conducted using an ABI7500 qPCR instrument (7900, Applied Biosystems, Carlsbad, CA, USA) and GAPDH was used as an internal control. The reaction conditions were as follows: 95 °C for 3 min. 95 °C for 3 s, 60 °C for 30 s, 95 °C for 15 s, 60 °C for 15 s, 95 °C for 15 s for a total of 40 cycles. The $2^{-\Delta\Delta Ct}$ method ($\Delta\Delta CT = \Delta Ct_{theexperimentgroup} - \Delta Ct_{thecontrolgroup}$) was employed to calculate the mRNA expression of ZO-1, occludin, claudin-5. The experiment was repeated 3 times.

Double-label immunofluorescence staining

To explore the distribution of DDAH-1 and its co-expression with endothelial cells and neurons in the brain, double-label immunofluorescence staining between DDAH-1 and endothelial cell/neuron was performed. The brain frozen sections of WT rats were obtained and processed as described above with some exceptions: the sections were incubated with 4 pairs of primary antibodies (DDAH-1, SantaCruz, 1:100; CD31, abcam,1:30; NeuN, abcam, 1:500; β-tubulin, abcam, 1:1000) and corresponding secondary antibodies respectively. Sections were viewed and photographed at a magnification of ×200 and ×400.

Statistical analysis

All data were shown as mean ± standard deviation and were analyzed using the SPSS version 22.0. Data sets were tested for equal variances using the Levene's test. Differences among groups were analyzed using one-way analysis of variance (ANOVA) and Kruskal–Wallis ANOVA, with LSD test for post hoc comparisons. $P < 0.05$ was considered statistically significant and designation included $^{*}p < 0.05$, $^{**}p < 0.01$, $^{***}p < 0.001$ in comparison.

Results

DDAH-1 main distribution in cerebral cortex, basal nuclei, neurons and endothelial cells

To clarify the distribution of DDAH-1 and its function, double-label immunofluorescence staining between DDAH-1 and endothelial cell/neuron was performed in different regions of the brain. A higher distribution of DDAH-1 was observed in the cerebral cortex and basal nuclei compared to brainstem and cerebellum (Fig. 1a), while DDAH-$1^{-/-}$ totally abolished DDAH-1 protein expression in brain tissues (Fig. 1b). DDAH-$1^{-/-}$ rats showed no detectable defect in development and growth, which was consistent with the prior observations in global DDAH-$1^{-/-}$ strain [32]. DDAH-$1^{-/-}$ also had no evident effect on the general appearance of cerebral vessels (Table S2).

In addition, DDAH-1 was mainly expressed in the endothelial cells (cerebral vessels) and neurons (Fig. 2). These data suggested that DDAH-1 may have a role in the regulation of endothelial cells and neurons.

DDAH1$^{-/-}$ has no detectable effect on cell death in rats under control conditions

To explore the function of DDAH-1 in IS, we first detected whether DDAH-$1^{-/-}$ had effects on cell death under non-ischemic condition. No significant difference was found in infarct volume ($0.00 \pm 0.00\ mm^3$ (KO/SHAM) vs. $0.00 \pm 0.00\ mm^3$ (WT/SHAM), $p > 0.05$, $n = 5$) and neurological behavior (0.00 ± 0.00 (KO/SHAM) vs. 0.00 ± 0.00 (WT/

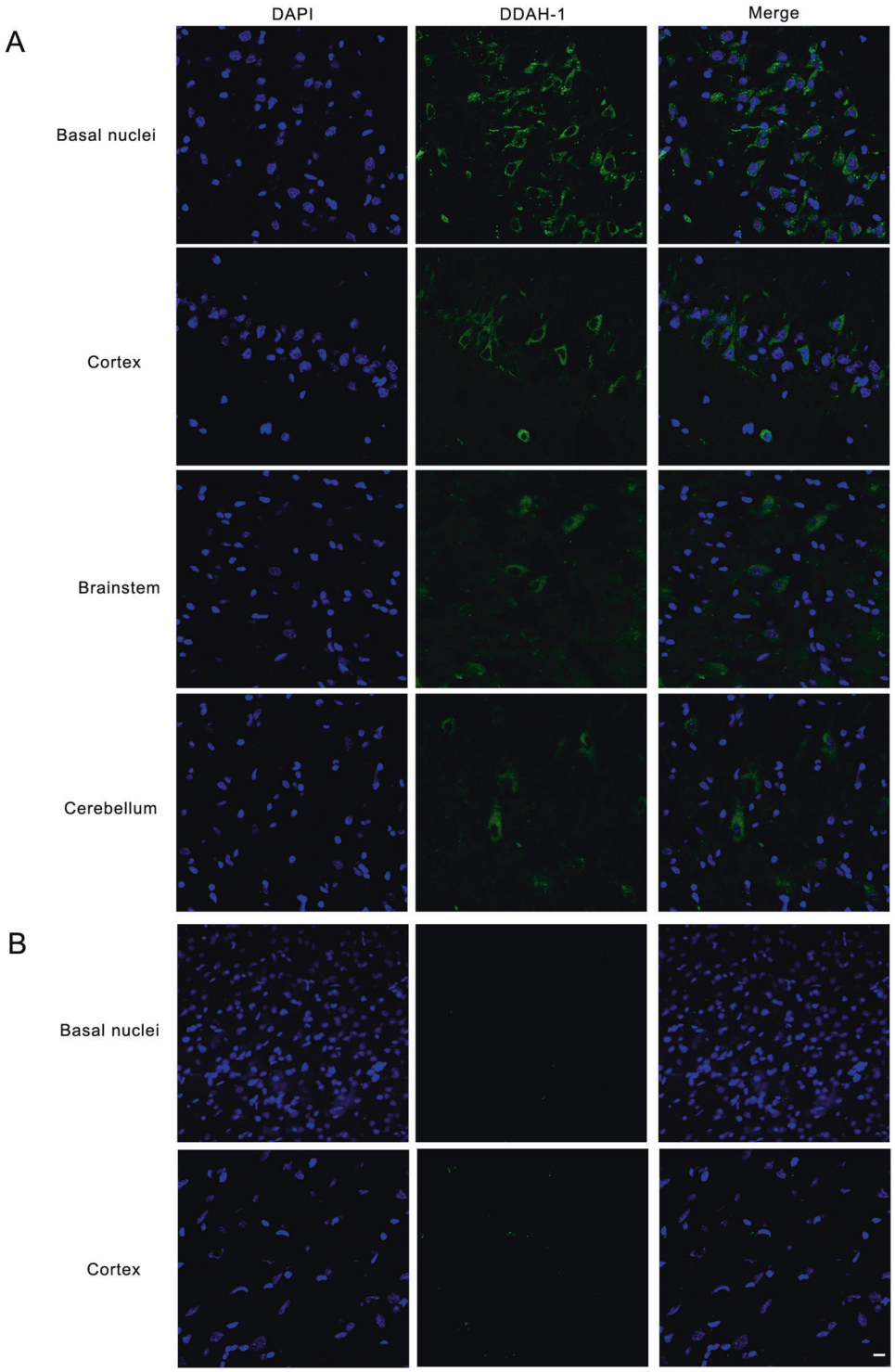

Fig. 1 Main distribution of DDAH-1 in basal nuclei, not brainstem. a DDAH-1 was distributed mainly in cerebral cortex and basal nuclei, but less in brainstem and cerebellum. Representative images of immunofluorescence staining for DDAH-1 in basal nuclei, cortex, brainstem and cerebellum were shown. **b** DDAH-$1^{-/-}$ totally abolished DDAH-1 protein expression in brain. Nearly no expression of DDAH-1 was exhibited in DDAH-$1^{-/-}$ rats brain. Representative images of immunofluorescence staining for DDAH-1 in basal nuclei and cortex were shown. Data were representative of 3 independent experiments. Magnification = ×200. scale bar = 10 μm. DAPI = 2-(4-Amidinophenyl)-6-indolecarbamidine dihydrochloride. DDAH-1 dimethylarginine dimethylamino hydrolase-1.

SHAM), $p > 0.05$, $n = 15$) between WT and DDAH-$1^{-/-}$ rats underwent SHAM operation (Fig. 3). There was also no significant difference in apoptosis cells number (173.4 ± 15.88 (KO/SHAM) vs. 170.6 ± 14.14 (WT/SHAM), $p > 0.05$, $n = 5$) and no clearly EBD extravasation (0.30 ± 0.05 μg/g (KO/SHAM) vs. 0.28 ± 0.06 μg/g (WT/SHAM), $p > 0.05$, $n = 5$) (Figs. 4 and 5).

Aggravated ischemic damage in DDAH-$1^{-/-}$ rats after MCAO/R model

The CBF and MABP were monitored before operation, after occlusion and reperfusion to evaluate the regulation of DDAH-1 on them. Values of MABP and alterations of CBF (% from baseline) are shown in Table S3. The MABP of

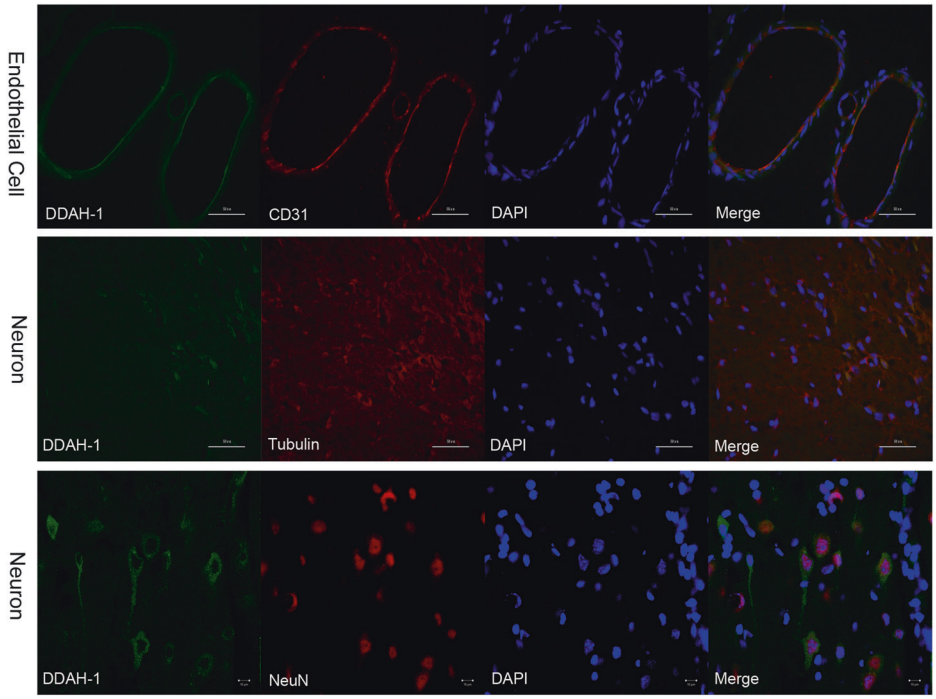

Fig. 2 Main distribution of DDAH-1 in neurons and endothelial cells. DDAH-1 was mainly co-localized with endothelial cells and neurons. Representative images of double-label immunofluorescence staining for DDAH-1 and CD31/Tubulin/NeuN were shown. Data were representative of 3 independent experiments. Magnification = ×200 and ×400, scale bar = 50 and 10 μm.

DDAH-1 KO rats was significantly increased compared to WT rats under normal condition (108.4 ± 0.87 mmHg (KO/SHAM) vs. 92.5 ± 1.22 mmHg (WT/SHAM), $p < 0.001$, $n = 15$). After MCAO/R model, both KO and WT rats showed increasing MABP, while MABP in KO rats significantly increased in comparison with WT rats (129.6 ± 0.89 mmHg (KO/M) vs. 115.6 ± 1.04 mmHg (WT/M), $p < 0.001$, $n = 15$). The CBF of KO rats at baseline were significantly lower than WT rats (−19.7 ± 1.52% (KO/SHAM) vs. 0 ± 0% (WT/SHAM), $p < 0.001$, $n = 15$). A 40–50% reduction of CBF was seen in WT rats after MCAO, and KO rats experienced a significantly higher reduction (−58.4 ± 1.61% (KO/M) vs. −45.2 ± 1.23% (WT/M), $p < 0.001$, $n = 15$). Following reperfusion both CBF of WT and KO rats significantly restored, while KO rats exhibited lower CBF in comparison with WT rats (−29.6 ± 1.45% (KO/M) vs. −16.9 ± 1.36% (WT/M), $p < 0.001$, $n = 15$).

Although there was no difference in cell death under SHAM operations, a significant increase in infarct volume at 24 h were found in the KO rats compared to WT rats after MCAO/R model (330.02 ± 12.16 mm^3 (KO/M) vs. 97.22 ± 8.73 mm^3 (WT/M), $p < 0.001$, $n = 5$) (Fig. 3a, c). For the percentage of infarct volume at 24 h, significant increase was also confirmed in KO rats (48.70 ± 1.16% (KO/M) vs. 13.59 ± 0.59% (WT/M), $p < 0.001$, $n = 5$) (Fig. 3d). Significant increase of NSS was found in KO group compared to WT group (14.1 ± 0.84 (KO/M) vs. 7.4 ± 0.63 (WT/M), $p = 0.039$, $n = 15$) (Fig. 3b).

In addition, significantly higher apoptotic cells number and rate were observed in the KO/M group (apoptotic number: 3060 ± 145.6, $p < 0.001$, apoptotic rate: 70.68 ± 5.72%, $p < 0.001$, $n = 5$) than WT/M group (apoptotic number: 1573 ± 168.1, apoptotic rate: 35.23 ± 1.77%, $p < 0.001$, $n = 5$) (Fig. 4).

To investigate whether DDAH-1 affects BBB during IS, we examined EBD extravasation as a marker of BBB disruption, as EBD usually binds to serum albumin and extravasates into brain tissue only when BBB is disrupted. Although no clearly EBD extravasation was shown in DDAH-$1^{-/-}$ rats under SHAM operation, DDAH-1 KO rats (2.4 ± 0.12 μg/g) were exhibited significant increase compared to WT rats (1.27 ± 0.07 μg/g) after MCAO/R ($p < 0.001$, $n = 5$) (Fig. 5).

Thus, these results indicated that the lack of DDAH-1 led to worse ischemic damage after MCAO/reperfusion, which suggests DDAH-1 might play a role in protecting from IS.

Close association of ADMA and NO level with neurological damages

To clarify whether DDAH-1 functions relying on NO, the peripheral blood ADMA levels, the NO concentrations and ADMA levels in infarct area were detected. ADMA in peripheral blood were significantly increased in DDAH-$1^{-/-}$ rats compared to WT rats both under normal (KO/SHAM: 105.72 ± 5.25 nmol/L vs. WT/SHAM: 42.59 ± 2.67 nmol/L, $p < 0.001$, $n = 5$) and ischemic conditions (KO/SHAM: 153.17 ± 9.11 nmol/L vs. WT/SHAM: 98.15 ± 3.8 nmol/L, $p < 0.001$, $n = 5$), and DDAH-$1^{-/-}$ rats with MCAO/R model were exhibited increasing ADMA

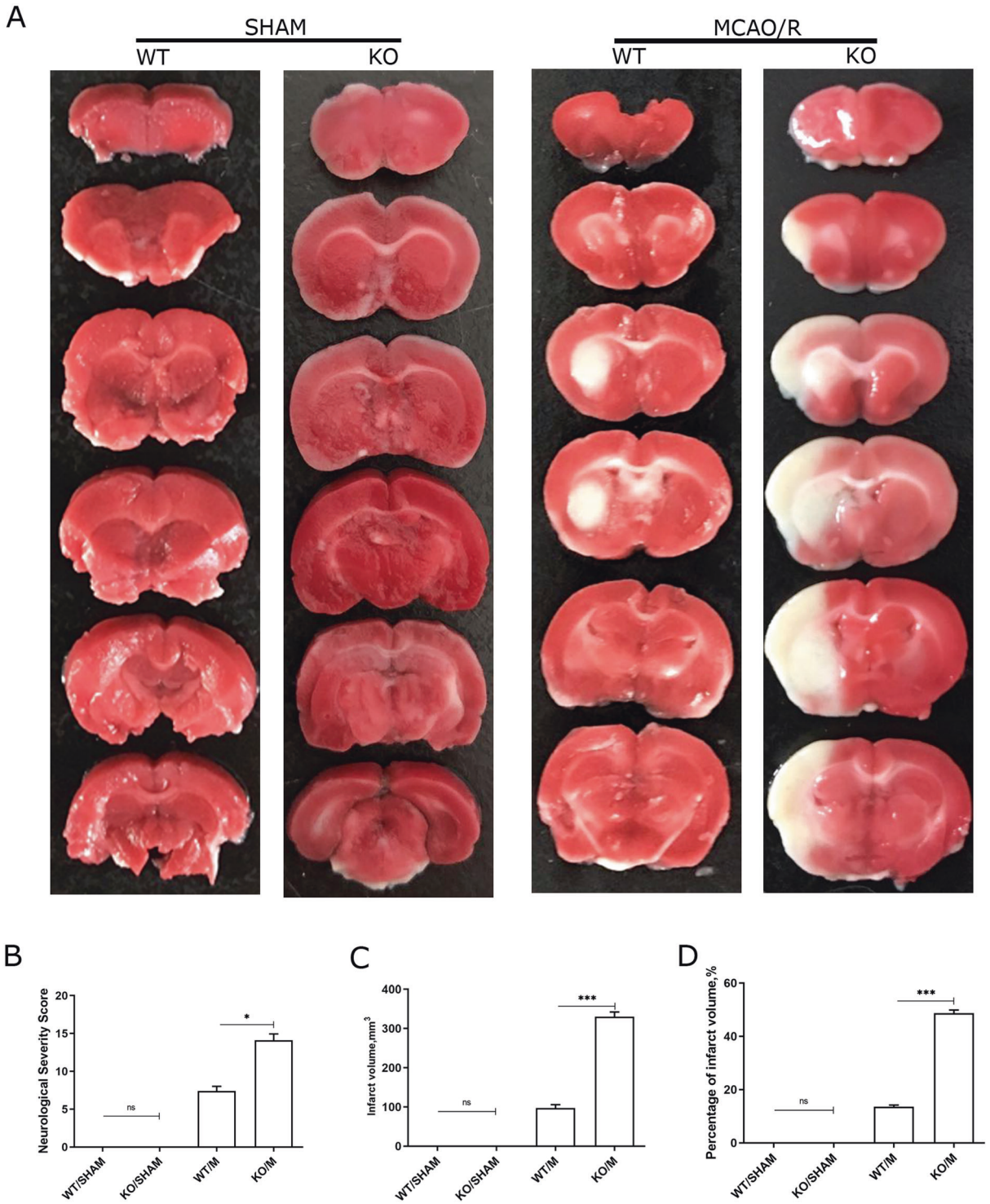

Fig. 3 DDAH-1$^{-/-}$ rats showed aggravated ischemic damage after MCAO/R. a Representative 24-h TTC staining of rat brain sections in DDAH-1$^{-/-}$ and WT rats under normal and ischemic conditions. The white-colored areas represented infarct region in these sections, and red-colored areas represented normal region. **b–d** Statistic analysis of NSS, infarct volume and its percentage. No significant difference was found in infarct volume and neurological behavior between WT and DDAH-1$^{-/-}$ rats under non-ischemic conditions ($n = 5$, $p > 0.05$). There were significant increases of NSS ($n = 15$, $p = 0.039$), infarct volume and percentage ($n = 5$, $p < 0.001$) in KO/M group. Data are presented as mean ± SD. $^{ns}p > 0.05$, $^{*}p < 0.05$, $^{***}p < 0.001$. KO knockout, WT wild-type, NSS neurological severity scores, MCAO/R middle cerebral artery occlusion/reperfusion.

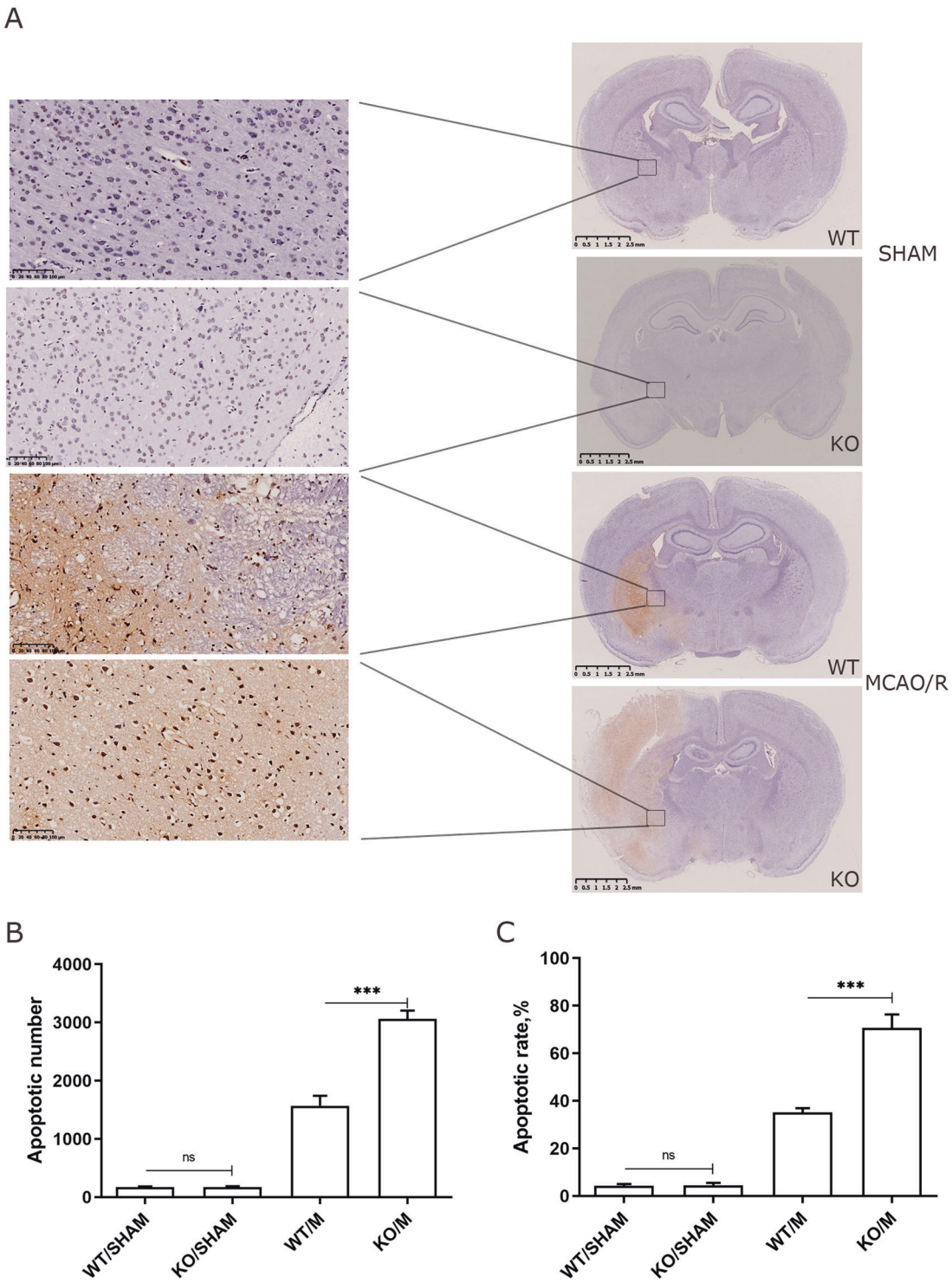

Fig. 4 DDAH-1$^{-/-}$ rats showed severer apoptosis in brain after MCAO/R. a Representative images of TUNEL assay in DDAH-1$^{-/-}$ and WT rats under normal and ischemic conditions. Apoptosis cells were shown as brown nucleus and normal cells was blue. **b**, **c** Statistic analysis of the apoptotic numbers and rates. No significant difference was found in apoptosis cells number and rate between DDAH-1$^{-/-}$ and WT rats under normal conditions ($n = 5$, $p > 0.05$), while after MCAO/R DDAH-1 KO rats exhibited a significantly increased number and rate ($n = 5$, $p < 0.001$). Data are presented as mean ± SD. $^{ns}p > 0.05$, $^{***}p < 0.001$. KO knockout, WT wild-type, MCAO/R middle cerebral artery occlusion/reperfusion.

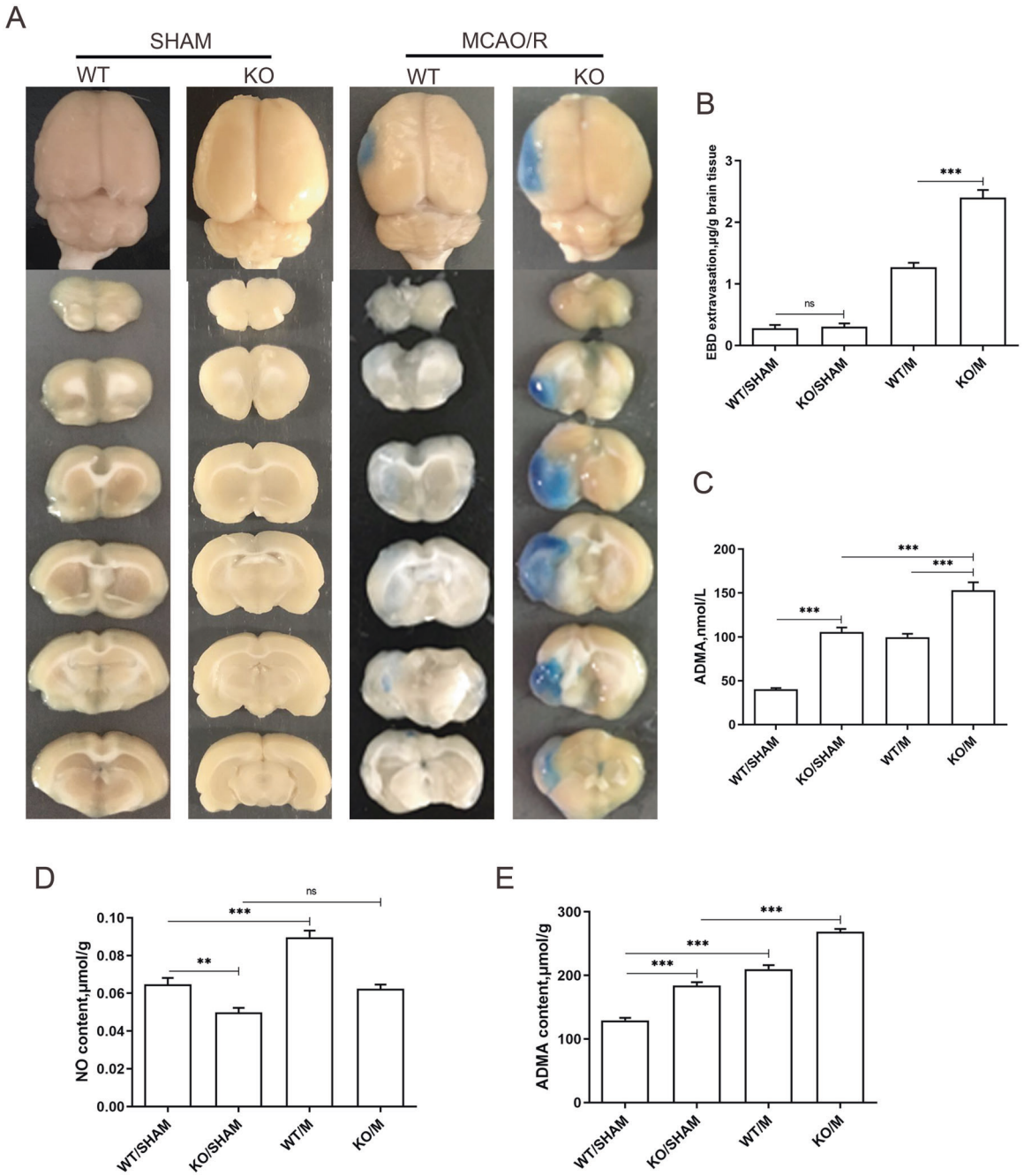

Fig. 5 DDAH-1$^{-/-}$ rats showed increased EBD extravasation after MCAO/R with lower NO and higher ADMA levels. a Representative sections of EBD extravasation in DDAH-1$^{-/-}$ and WT rats under normal and ischemic conditions. The blue areas represented the extravasation of EBD. **b** Statistic analysis of EBD extravasation. Under normal condition, there was no significant difference between KO and WT rats ($n = 5$, $p > 0.05$). After MCAO/R model, KO rats showed a significantly higher extravasation ($n = 5$, $p < 0.001$). **c–e** Statistic analysis of brain NO, ADMA and plasma ADMA levels. ADMA in peripheral blood and brain were significantly increased in DDAH-1$^{-/-}$ rats compared to WT rats both under normal and ischemic conditions ($n = 5$, $p < 0.001$). The ADMA levels in both KO and WT rats significantly increased after MCAO/R model ($n = 5$, $p < 0.001$). The NO levels were significantly decreased in DDAH-1$^{-/-}$ rats ($n = 5$, $p < 0.01$). The NO concentration in WT rats significantly increased after MCAO/R, while no significant difference was shown between KO/SHAM and KO/M group ($n = 5$, $p > 0.05$). Data are presented as mean ± SD. $^{ns}p > 0.05$, $^{**}p < 0.01$, $^{***}p < 0.001$. KO knockout, WT wild-type, EBD Evan's blue dye, MCAO/R middle cerebral artery occlusion/reperfusion, NO nitric oxide, ADMA asymmetric dimethylarginine.

levels in peripheral blood compared to DDAH-1$^{-/-}$ rats with SHAM operation ($p < 0.001$, $n = 5$) (Fig. 5c).

The NO concentrations in infarct area were demonstrated to significantly decrease in DDAH-1$^{-/-}$ rats (0.05 ± 0.002 μmol/g) compared to WT rats (0.07 ± 0.003 μmol/g) under non-ischemic conditions ($p = 0.0076$, $n = 5$). After MCAO/R model, WT rats showed significant increase in NO concentration (0.09 ± 0.003 μmol/g, $p < 0.001$, $n = 5$). NO content in DDAH-1$^{-/-}$ rats increased after MCAO/R, but not significant (0.06 ± 0.002 μmol/g, $p = 0.0562$, $n = 5$) (Fig. 5d). As expected, ADMA levels of infarct area in DDAH-1$^{-/-}$ rats significantly increased compared to WT rats both under non-ischemic (KO/SHAM: 184.23 ± 5.18 μmol/g vs. WT/SHAM: 129.49 ± 3.80 μmol/g, $p < 0.001$, $n = 5$) and ischemic conditions (KO/SHAM: 268.79 ± 4.44 μmol/g vs. WT/SHAM: 209.79 ± 6.39 μmol/g, $p < 0.001$, $n = 5$). The MCAO/R model also led to a significant increase for ADMA level in infarct area tissue ($p < 0.001$, $n = 5$) (Fig. 5e).

L-Arginine supplementation to DDAH-1$^{-/-}$ rats restored ischemic damages

As ARG is the substrate for NO production, we then explored whether the supplement of ARG to DDAH-1$^{-/-}$ rats would improve the ischemic outcomes. As expected, ARG supplement significantly decreased NSS (ARG: 9.5 ± 1.15 vs. KO: 15.4 ± 1.03, $p < 0.001$, $n = 15$), infarct volume (ARG: 90.86 ± 19.42 mm^3 vs. KO: 358.7 ± 27.02 mm^3, $p < 0.001$, $n = 5$) infarct percentage (ARG: 9.99 ± 1.54% vs. KO: 25.58 ± 1.41%, $p < 0.001$, $n = 5$) and apoptotic cell number (ARG: 1763 ± 143.2 vs. KO: 3046 ± 186.3, $p < 0.001$, $n = 5$) at 24 h, meanwhile ARG group had no significant difference with WT group (NSS: 8.9 ± 0.88, $p = 0.632$, infarct volume: 92.8 ± 11.42 mm^3, $p = 0.998$, infarct percentage: 8.268 ± 0.79%, $p = 0.127$, apoptotic cell number: 1573 ± 126.5, $p = 0.129$) (Fig. 6).

For the BBB disruption, ARG supplementation (1.42 ± 0.12 μg/g) significantly decreased EBD extravasation in KO rats (2.4 ± 0.12 μg/g) ($p < 0.001$, $n = 5$), while there was no significant difference between ARG and WT group (1.31 ± 0.13 μg/g) ($p = 0.308$, $n = 5$) (Fig. 6c, h).

Long-term (3 and 7-days) ischemic outcomes were also assessed in this study. For infarct volume, there were significant increase in KO rats compared to WT rats both at 3rd (102.3 ± 7.26 mm^3 (KO) vs. 65.85 ± 4.37 mm^3 (WT), $p < 0.001$, $n = 5$) and 7th day (71.4 ± 3.94 mm^3 (KO) vs. 37.44 ± 3.49 mm^3 (WT), $p < 0.001$, $n = 5$) (Fig. 7a, b, d). Consistently, the percentage of infarct volume and NSS also showed significant increase in KO rats both at 3rd (infarct percentage: 8.26 ± 0.52% (KO) vs. 5.43 ± 0.61% (WT), $p < 0.001$, $n = 5$; NSS: 7.3 ± 0.48 (KO) vs. 3.8 ± 0.41 (WT), $p < 0.001$, $n = 15$) and 7th day (infarct percentage: 5.48 ± 0.72% (KO) vs. 2.81 ± 0.62% (WT), $p < 0.001$, $n = 5$; NSS: 3.9 ± 0.73 (KO) vs. 1.2 ± 0.63 (WT), $p < 0.001$, $n = 15$) after MCAO/R (Fig. 7c, e). ARG supplement significantly decreased the infarct volume (3-day: 64.35 ± 4.828 mm^3, 7-day: 37.55 ± 2.691 mm^3, $n = 5$), infarct percentage (3-day: 5.05 ± 0.143%, 7-day: 3.16 ± 0.396%, $n = 5$) and NSS (3-day: 3.4 ± 0.29, 7-day: 1.3 ± 0.43, $n = 15$) both at 3rd and 7th day in DDAH-1$^{-/-}$ rats ($p < 0.001$), while there was no significant difference between ARG and WT group ($p > 0.05$) (Fig. 7).

Enhanced TJ proteins degradation in DDAH-1$^{-/-}$ rats

To further explore the molecular mechanism, the expressions and mRNA levels of TJ related proteins zonula occludens 1 (ZO-1), occludin and claudin-5 were measured using western blot and RT-qPCR (Fig. 8). Interestingly, under normal conditions the expression of ZO-1, occludin and claudin-5 significantly decreased in DDAH-1$^{-/-}$ rats (ZO-1: 0.719 ± 0.018, occludin: 0.911 ± 0.023, claudin-5: 0.713 ± 0.078) compared to WT rats (ZO-1: 0.971 ± 0.047, occludin: 1.114 ± 0.087, claudin-5: 0.974 ± 0.059) ($p < 0.001$, $n = 5$). After ARG supplementation, the expression of ZO-1, occludin and claudin-5 significantly increased in DDAH-1$^{-/-}$ rats (ZO-1: 0.871 ± 0.02, occludin: 1.042 ± 0.075, $p < 0.001$; claudin-5: 0.873 ± 0.028, $p = 0.0164$, $n = 5$), and no significant difference was shown in occludin and claudin-5 compared with WT rats (occludin: 1.046 ± 0.052, $p = 0.769$; claudin-5: 0.977 ± 0.049, $p = 0.092$, $n = 5$). Under ischemic conditions, both WT and KO rats showed decreased expression of TJ proteins, and the expression in KO rats (ZO-1: 0.239 ± 0.020, occludin: 0.3202 ± 0.015, claudin-5: 0.223 ± 0.011) was significantly lower than WT rats (ZO-1: 0.4624 ± 0.032, occludin: 0.592 ± 0.053, claudin-5: 0.451 ± 0.021) ($p < 0.001$, $n = 5$). Then, we supplemented ARG to these rats underwent MCAO/R and found the expression of TJ proteins significantly increased in both WT (ZO-1: 0.669 ± 0.016, occludin: 0.795 ± 0.014, claudin-5: 0.702 ± 0.022) and DDAH-1$^{-/-}$ rats (ZO-1: 0.509 ± 0.016, occludin: 0.605 ± 0.022, claudin-5: 0.456 ± 0.059) ($p < 0.001$, $n = 5$). Also, the supplement of ARG to DDAH-1$^{-/-}$ rats was exhibited similar expressions with WT/M rats (ZO-1: $p = 0.704$, occludin: $p = 0.713$, claudin-5: $p > 0.99$, $n = 5$) (Fig. 8a–d).

However, the mRNA levels of TJ proteins (normalized to WT/SHAM group) were not significantly different in these groups ($p > 0.05$, $n = 5$) (Fig. 8e), suggesting that the decrease of TJ proteins may result from an effect downstream of transcription such as protein degradation.

To sum up, the supplementation of L-arginine to DDAH-1$^{-/-}$ rats partially reversed the neurological damages and reductions of TJ protein expression, which suggests that DDAH-1 might regulate the degradation of TJ protein and protect from ischemia-induced BBB disruption.

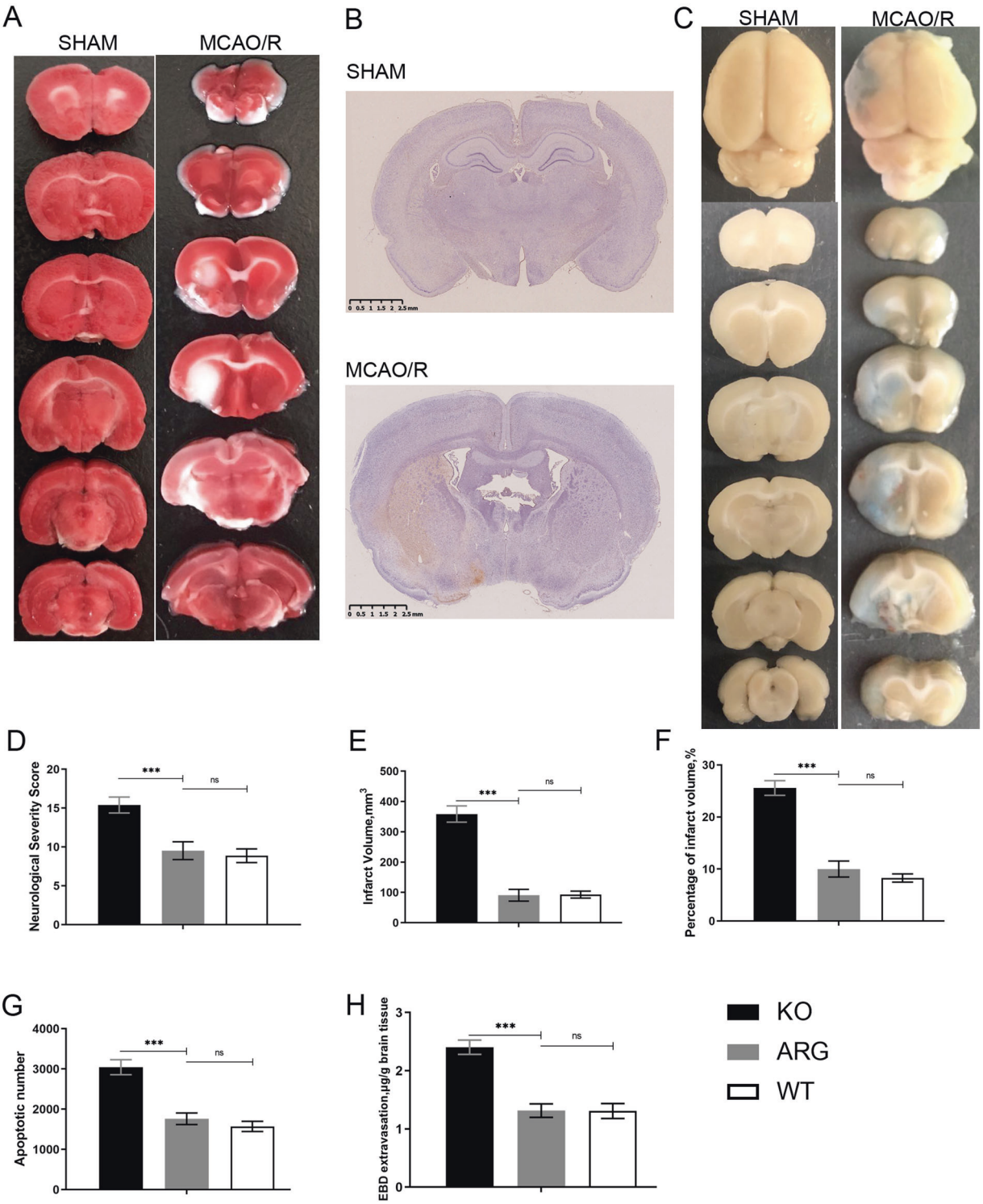

Fig. 6 Supplement of L-arginine to DDAH-1$^{-/-}$ rats alleviated partial neurological damages. a Representative 24-h TTC staining for DDAH-1$^{-/-}$ rats with ARG supplementation under normal and ischemic conditions. **b** Representative images of TUNEL assay in DDAH-1$^{-/-}$ rats with ARG supplementation under normal and ischemic conditions. **c** Representative sections of EBD extravasation in DDAH-1$^{-/-}$ rats with ARG supplementation under normal and ischemic conditions. **d–h** Statistic analysis of NSS, infarct volume, infarct percentage, apoptotic number and EBD extravasation. ARG supplement significantly decreased NSS, infarct volume, infarct percentage, apoptotic number and EBD extravasation ($p < 0.001$), but exhibited no significant difference with WT rats ($p > 0.05$). Data are presented as mean ± SD. $^{ns}p > 0.05$, $^{***}p < 0.001$. KO knockout, WT wild-type, EBD Evan's blue dye, MCAO/R middle cerebral artery occlusion/reperfusion, ARG L-arginine.

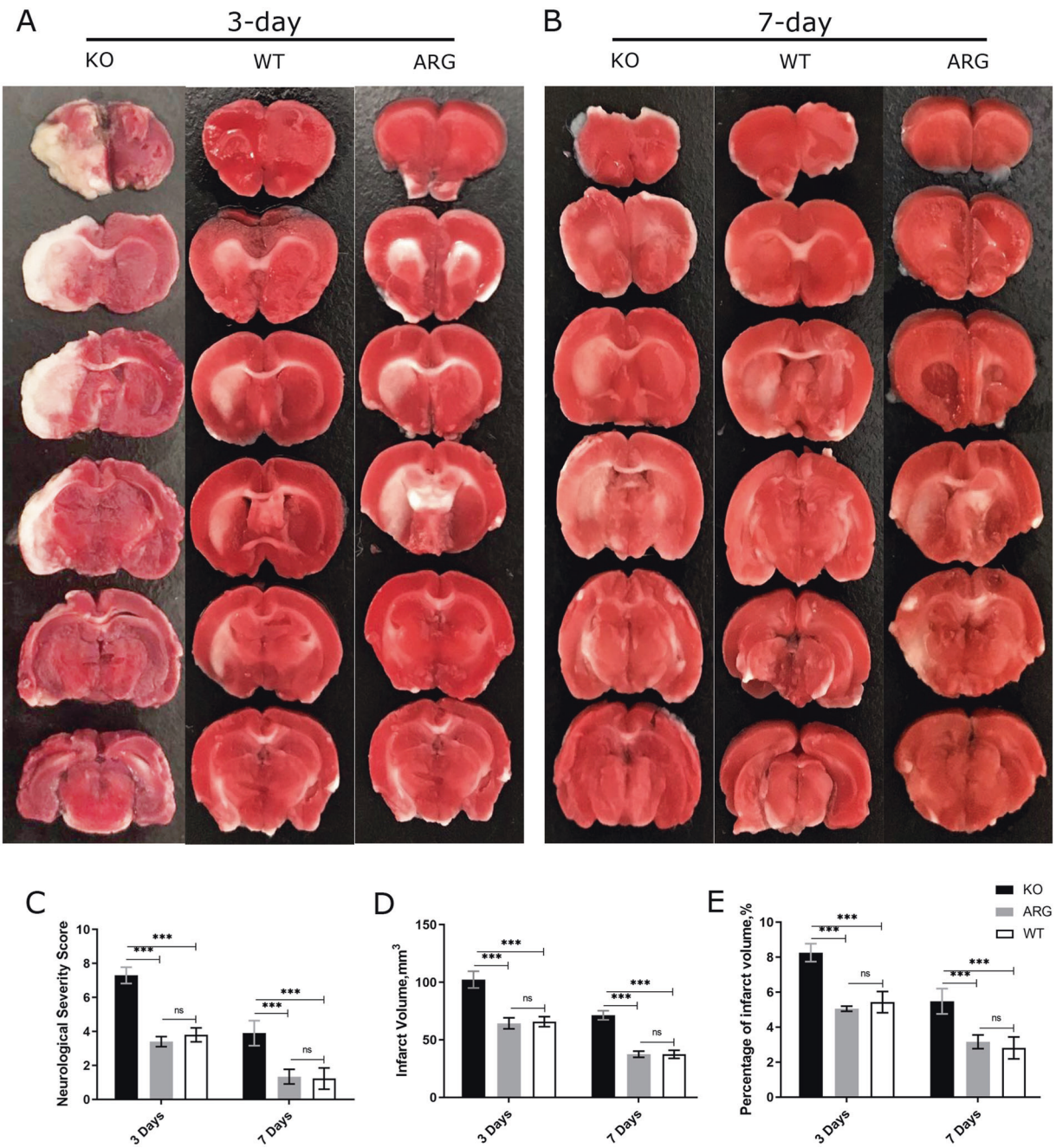

Fig. 7 Supplement of L-arginine to DDAH-1$^{-/-}$ rats relieved long-term neurological damages. a, **b** Representative 3 and 7-day TTC staining for DDAH-1 KO, WT group and ARG group. **c–e** Statistic analysis of infarct volume and its percentage in 3 and 7 days. There were significant increases of infarct volume, infarct percentage and NSS in the KO group compared to the other groups both in 3 and 7 days ($p < 0.001$), but no significant difference between WT and ARG group ($p > 0.05$). Data are presented as mean ± SD. $^{ns}p > 0.05$, $^{***}p < 0.001$. KO knockout, WT wild-type, ARG L-arginine, NSS neurological severity scores.

Discussion

Previous studies have demonstrated that ADMA is strongly correlated with IS, as well as with many other vascular-related diseases [11]. Over recent years, numerous DDAH-1 related data have emerged, highlighting its role in various diseases, and especially in cardiovascular conditions. Nonetheless, the function of DDAH-1 in IS and underlying mechanisms still remain unknown. In the present study, we demonstrated that DDAH-1 was mainly distributed in cerebral cortex and basal nuclei and was largely expressed in endothelial cells and neurons. It negatively regulated IS pathogenesis, probably via NO signaling and decreasing ADMA level also preventing tight junction degradation.

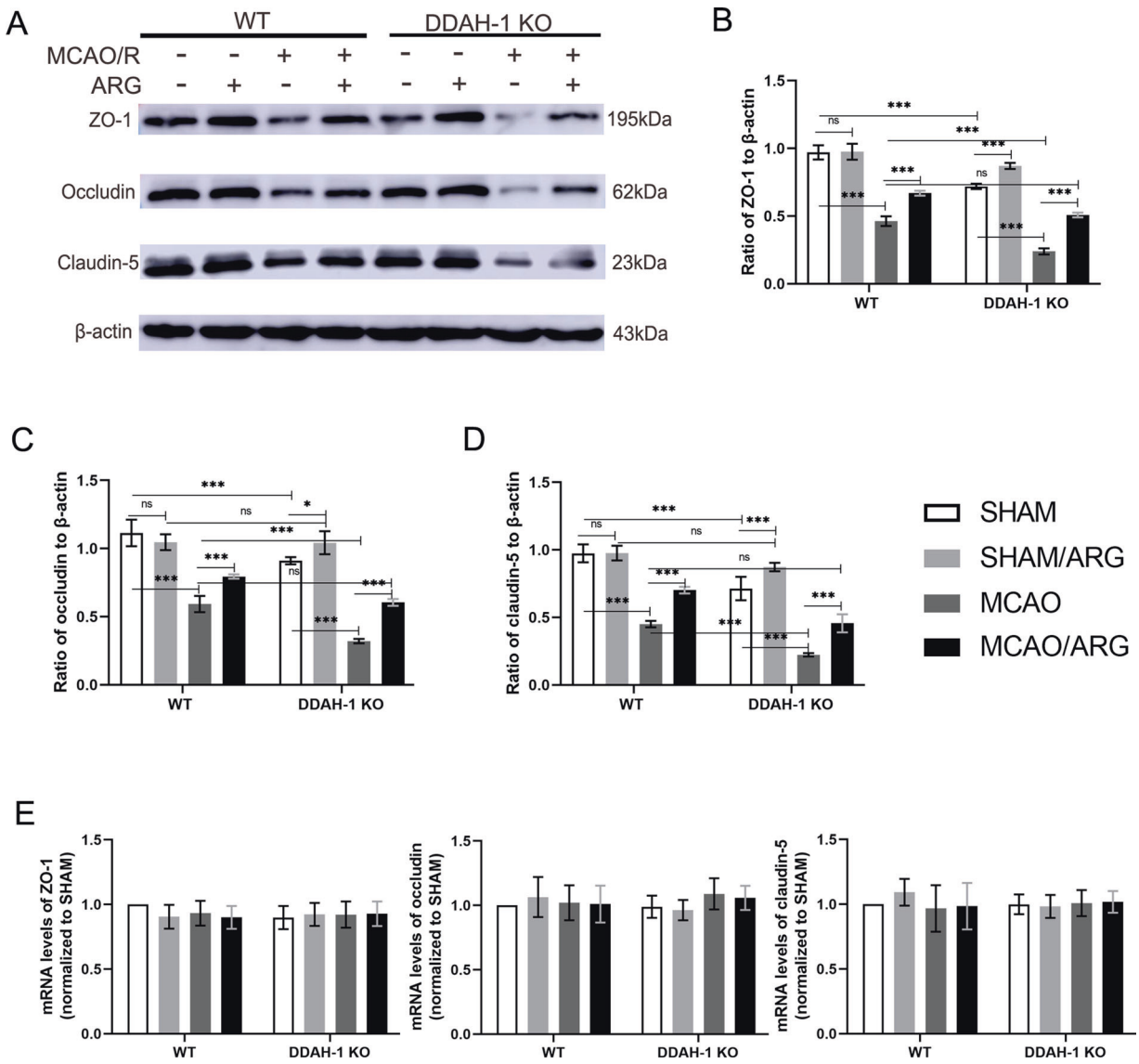

Fig. 8 DDAH-1$^{-/-}$ rats showed decreased expressions of tight junction proteins. a Representative western blots of ZO-1, occludin, and claudin-5. **b–d** Statistic analysis and quantification respectively. Under normal condition, the expression of ZO-1, occludin and claudin-5 significantly decreased in DDAH-1$^{-/-}$ rats compared to WT rats ($n = 5$, $p < 0.001$). After ARG supplementation, the expression of ZO-1, occludin and claudin-5 significantly increased ($n = 5$, $p < 0.001$). Under ischemic conditions, the expression of tight junction proteins in both WT and KO rats decreased ($n = 5$, $p < 0.001$), and the expression in KO rats was significantly lower than WT rats ($n = 5$, $p < 0.001$). Also, the ARG supplement increased the expression of tight junction proteins both in KO and WT rats ($n = 5$, $p < 0.001$). **e** Statistic analysis and quantification of mRNA levels respectively. The mRNA levels of TJ proteins (normalized to SHAM group) showed no significant difference in these groups ($n = 5$, $p > 0.05$). Data are presented as mean ± SD. $^{ns}p > 0.05$, $^{*}p < 0.05$, $^{***}p < 0.001$. KO knockout, WT wild-type, ARG L-arginine, MCAO/R middle cerebral artery occlusion/reperfusion, DDAH-1 dimethylarginine dimethylamino hydrolase-1, ZO-1 zonula occludens 1.

DDAH-1 dysfunction has been implicated in several cardiovascular conditions, such as hypertension, coronary heart disease and congestive heart failure [33]. Treatment based on DDAH-1 has been used in acute congestive heart failure to decrease ADMA levels [25]. It has also shown the ability to reduce portal pressure via ADMA-mediated regulation of NOS activity and it has shown connection with intracerebral hemorrhage through NO signaling [4, 24]. A clinical study has shown that DDAH-1 loss-of-function polymorphism is associated with both increased risk of thrombosis stroke and coronary heart disease [22]. We recently demonstrated that DDAH-1 could regulate the levels of ADMA and NO and enhances the ischemic tolerance in hypoxic preconditioning [34].

In the beginning of our study, we observed high distribution of DDAH-1 in cerebral cortex and basal nuclei, as well as high expression in endothelial cells and neurons, which indicated its possibility correlating to IS. MCAO/R

model was used to mimic IS pathogenesis in human. Neurological score, TTC staining and TUNEL assay were examined to evaluate the brain injury. Under non-ischemic conditions, no detected brain damage was found in DDAH-$1^{-/-}$ rats compared with WT rats. However, after MCAO/R we found that DDAH-$1^{-/-}$ rats showed worse behavior, larger infarct volume and higher cell apoptosis, thus suggesting an aggravated damage compared to WT rats, which indicated that DDAH-1 had a protective role in IS. ADMA was reported to lower cerebral perfusion and increases arterial stiffness both in animals and humans [35–37]. In our study, DDAH-1 KO rats exhibited decreasing CBF and increasing MABP compared to WT rats, both at baseline and during MCAO/R period. As no brain injury including BBB disruption was found in KO rats under normal conditions, the lower CBF in DDAH-$1^{-/-}$ rats might not be the primary cause for BBB leakage.

Low level of NO is responsible for vasoconstriction and vascular closure thus leading to worse pathology in IS, worse neurological function, larger infarct area and enhanced apoptosis [5, 6, 38]. Endogenous level of NO in the brain is increased following stroke and animal stroke models using MCAO/R procedures [39]. High concentrations of ADMA are also present in cardiovascular and cerebrovascular events [40, 41]. In this study, increasing NO level was found in brain after MCAO/R as a protective effect, while lower NO level was shown in DDAH-$1^{-/-}$ rats compared to WT rats. We also found higher levels of peripheral blood and brain ADMA in DDAH-$1^{-/-}$ rats both under non-ischemic and ischemic conditions, indicating DDAH-1 could protect IS-induced pathology via regulating ADMA and NO levels.

In previous studies, the supplement of NO from L-arginine restored vascular function and improved clinical symptoms in various diseases [42, 43]. DDAH-$1^{-/-}$ rats were also exhibited improved pathology and partial restoration of neurological damages following L-arginine supplementation in our study. The restoration by NO further confirmed the role of DDAH-1 in IS via NO signaling.

BBB has a dynamic structure that contributes to cerebral homeostasis. It is composed of endothelial cells and their linking TJ, pericytes, astrocytic end feet and extracellular matrix components and is believed to be disrupted in IS pathogenesis [44–47]. Herein, we examined BBB permeability via EBD extravasation and TJ proteins expression [48]. EBD which binds to serum albumin and IgG does not cross into brain parenchyma from vascular tissue due to their high molecular weight [49, 50]. TJ disruption is a major cause underlying increased permeability of BBB after IS and TJ is regulated physiologically and pathophysiologically by TJ protein modification, translocation and degradation [44, 51]. Seungho et al. found that ADMA treatment exacerbated blood-brain barrier dysfunction and loss of TJ proteins [52]. ADMA was also reported to have potent adverse effects on the TJ protein occludin [53]. In our study, DDAH-$1^{-/-}$ rats showed higher leakage of EBD in brain parenchyma and lower expression of TJ proteins after MCAO/R, which suggested enhanced BBB damage in DDAH-$1^{-/-}$ rats; while the supplementation with L-arginine partly restored that damage. Interestingly, we found that even under non-ischemic conditions, DDAH-1 depletion significantly decreased the expression of TJ protein. However, the mRNA levels of TJ proteins remained unchanged in these groups. It indicated that DDAH-1 exerts its protective role in BBB, not only through promoting endothelial cells homeostasis but may also via preventing TJ protein degradation. DDAH-1 deficiency reduces NO production via DDAH-ADMA-NOS axis in endothelial cells, leading to endothelial dysfunction and death, and subsequent dysregulation of ionic homeostasis, degradation of TJ proteins which further impairs the BBB permeability [3].

We also performed preliminary experiment and an informal interim assessment through the experiment, by which could largely reduce animal use. This approach follows the guidelines of the National Centre for the Replacement, Refinement and Reduction of Animals in Research (London, UK).

In conclusion, our study demonstrated that DDAH-1 have a vital protective role in IS via regulating ADMA level and possibly via preventing TJ proteins degradation. Supplementation with L-arginine may help restore some of the functions in DDAH-$1^{-/-}$ rats. In future studies our research provides novel insight into DDAH-1 that can be used as a novel therapeutic target for IS and a pharmacological target for BBB permeability.

Acknowledgements DDAH-1 knockout SD rats were provided by Professor Da-Chun Xu (Department of Cardiology, Shanghai Tenth People's Hospital, Tongji University School of Medicine).

Funding The present study was supported by the Science and Technology Commission of Shanghai Municipality (grant numbers 18140901900 and 20ZR1443500), National Natural Science Foundation of China (Grant no. 8207052336), and Shanghai Municipal Key Clinical Specialty (Grant no. shslczdzk06102).

Compliance with ethical standards

Conflict of interest The authors declare that they have no conflict of interest.

References

1. Katan M, Luft A. Global burden of stroke. Semin. Neurol. 2018; 38:208–11.

2. Wang W, Jiang B, Sun H, Ru X, Sun D, Wang L, et al. Prevalence, incidence, and mortality of stroke in China. Circulation. 2017;135:759.
3. Chung JW, Oh MJ, Cho YH, Moon GJ, Kim GM, Chung CS, et al. Distinct roles of endothelial dysfunction and inflammation in intracranial atherosclerotic stroke. Eur. Neurol. 2017;77:211–9.
4. Na L, Hans W, Milani D, Shufen C, Karin W. Nitric oxide (NO) and asymmetric dimethylarginine (ADMA): their pathophysiological role and involvement in intracerebral hemorrhage. Neurol. Res. 2011;33:541–8.
5. Patrick V, James L, Blocking NO. synthesis: how, where and why? Nat. Rev. Drug Discov. 2002;1:939–50.
6. Nadja S, Anja S, Jens ML, Thomas K, Gulistan T, Thomas L, et al. Endothelial dysfunction of the peripheral vascular bed in the acute phase after ischemic stroke. Cerebrovasc. Dis. 2012;33: 37–46.
7. Leiper J, Nandi M, Torondel B, Murray-Rust J, Malaki M, O'Hara B, et al. Disruption of methylarginine metabolism impairs vascular homeostasis. Nat. Med. 2007;13:198–203.
8. Pope AJ, Karrupiah KP. Role of dimethylarginine dimethylaminohydrolases in the regulation of endothelial nitric oxide production. J. Biol. Chem. 2009;284:35338–47.
9. Pope AJ, Karuppiah K, Cardounel AJ. Role of the PRMT–DDAH–ADMA axis in the regulation of endothelial nitric oxide production. Pharmacol. Res. Off. J. Ital. Pharmacol. Soc. 2009;60:461–5.
10. Zhang Y, Fan D, Zhang N. The relationship between serum asymmetric dimethylarginine and ABCD2 score in transient ischemic attack patients. Zhonghua NeiKe ZaZhi. 2014;53:876–9.
11. Chen S, Li N, Deb-Chatterji M, Dong Q, Kielstein JT, Weissenborn K, et al. Asymmetric dimethyarginine as marker and mediator in ischemic stroke. Int. J. Mol. Sci. 2012;13:15983.
12. Greco R, Ferrigno A, Demartini C, Zanaboni A, Mangione AS, Blandini F, et al. Evaluation of ADMA-DDAH-NOS axis in specific brain areas following nitroglycerin administration: study in an animal model of migraine. J. Headache Pain. 2015;16:74.
13. Molnar T, Pusch G, Nagy L, Keki S, Berki T, Illes Z. Correlation of the L-arginine pathway with thrombo-inflammation may contribute to the outcome of acute ischemic stroke. J. Stroke Cerebrovasc. Dis. 2016;25:2055–60.
14. Nakayama Y, Ueda S, Yamagishi SI, Obara N, Taguchi K, Ando R, et al. Asymmetric dimethylarginine accumulates in the kidney during ischemia/reperfusion injury. Kidney Int. 2014;85:570–8.
15. Segarra G, Cortina B, Mauricio MD, Novella S, Lluch P, Navarrete-Navarro J, et al. Effects of asymmetric dimethylarginine on renal arteries in portal hypertension and cirrhosis. World J. Gastroenterol. 2016;22:10545–56.
16. Chih-Min T, Hsuan-Chang K, Chien-Ning H, Li-Tung H, You-Lin T. Metformin reduces asymmetric dimethylarginine and prevents hypertension in spontaneously hypertensive rats. Transl. Res. 2014;164:452–9.
17. Yokoro M, Nakayama Y, Yamagishi SI, Ando R, Sugiyama M, Ito S, et al. Asymmetric dimethylarginine contributes to the impaired response to erythropoietin in CKD-anemia. J. Am. Soc. Nephrol. 2017;28:2670.
18. Monti L, Morbidelli L, Bazzani L, Rossi A. Influence of circulating endothelin-1 and asymmetric dimethylarginine on whole brain circulation time in multiple sclerosis. Biomarker Insights. 2017;12:1177271917712514.
19. Chertow JH, Alkaitis MS, Nardone G, Ikeda AK, Cunnington AJ, Okebe J, et al. Plasmodium infection is associated with impaired hepatic dimethylarginine dimethylaminohydrolase activity and disruption of nitric oxide synthase inhibitor/substrate homeostasis. PLoS Pathog. 2015;11:e1005119.
20. Donia A, Anne M, Sabine GS, Monique P, Bernard B, Philippe V, et al. Cerebral changes occurring in arginase and dimethylarginine dimethylaminohydrolase (DDAH) in a rat model of sleeping sickness. Plos One. 2011;6:e16891.
21. Adel B, Oleg P, Ashraf T, Farid H, Ramadan H, Wiebke J, et al. Effects of dimethylarginine dimethylaminohydrolase-1 overexpression on the response of the pulmonary vasculature to hypoxia. Am J Respir Cell Mol Biol. 2013;49:491–500.
22. Hu D, Bin W, Hu W, Zhilan L, Jiangtao Y, Xiaojing W, et al. A novel loss-of-function DDAH1 promoter polymorphism is associated with increased susceptibility to thrombosis stroke and coronary heart disease. Circ. Res. 2010;106:1145–52.
23. Dê¼Mello R, Sand CA, Pezet S, Leiper JM, Gaurilcikaite E, Mcmahon SB, et al. Dimethylarginine dimethylaminohydrolase 1 is involved in spinal nociceptive plasticity. Pain. 2015;156: 2052–60.
24. Mookerjee RP, Gautam M, Vairappan B, Mohamed FEZ, Nathan D, Vikram S, et al. Hepatic dimethylarginine-dimethylaminohydrolase1 is reduced in cirrhosis and is a target for therapy in portal hypertension. J. Hepatol. 2015;62:325–31.
25. Speranza L, Franceschelli S, D'Orazio N, Gaeta R, Bucciarelli T, Felaco M, et al. The biological effect of pharmacological treatment on dimethylaminohydrolases (DDAH-1) and cationic amino acid transporter-1 (CAT-1) expression in patients with acute congestive heart failure. Microvasc. Res. 2011;82:391–6.
26. Bell T, Araujo M, Luo Z, Tomlinson J, Leiper J, Welch WJ, et al. Regulation of fluid reabsorption in rat or mouse proximal renal tubules by asymmetric dimethylarginine (ADMA) & dimethylarginine dimethylaminohydrolase (DDAH) 1. Am. J. Physiol. Renal Physiol. 2018;315:F74–8.
27. Shahin NN, Abdelkader NF, Safar MM. A novel role of irbesartan in gastroprotection against indomethacin-induced gastric injury in rats: targeting DDAH/ADMA and EGFR/ERK signaling. Sci Rep. 2018;8:4280.
28. Frank L, Chi-Un C, Mathias G, Eike-Christin VL, Dorothee A, Edzard S, et al. Dimethylarginine dimethylaminohydrolase-1 transgenic mice are not protected from ischemic stroke. Plos One. 2009;4:e7337.
29. Nannan C, Changhong S, Lu G, Dan Z, Xiufei X, Xiaojun Z, et al. Genome editing with RNA-guided Cas9 nuclease in zebrafish embryos. Cell Res. 2013;23:465–72.
30. Haley MJ, Lawrence CB. The blood-brain barrier after stroke: Structural studies and the role of transcytotic vesicles. J. Cereb. Blood Flow Metab. 2016;37:0271678X16629976.
31. Albert-Weißenberger C, Várrallyay C, Raslan F, Kleinschnitz C, Sirén AL. An experimental protocol for mimicking pathomechanisms of traumatic brain injury in mice. Exp. Transl. Stroke Med. 2012;4:1–5.
32. Wang D, Li H, Weir E, Xu Y, Xu D, Chen Y. Dimethylarginine dimethylaminohydrolase 1 deficiency aggravates monocrotaline-induced pulmonary oxidative stress, pulmonary arterial hypertension and right heart failure in rats. Int. J. Cardiol. 2019;295: 14–20.
33. Palm F, Onozato ML, Luo Z, Wilcox CS. Dimethylarginine dimethylaminohydrolase (DDAH): expression, regulation, and function in the cardiovascular and renal systems. Am. J. Physiol. Heart Circ. Physiol. 2007;293:H3227.
34. Zhao Y, Zhou Y, Ma X, Liu X, Zhao Y, Liu X. DDAH-1 via HIF-1 target genes improves cerebral ischemic tolerance after hypoxic preconditioning and middle cerebral artery occlusion-reperfusion. Nitric Oxide. 2020;95:17–28.
35. Kielstein JT, Donnerstag F, Gasper S, Menne J, Kielstein A, Martens-Lobenhoffer J, et al. ADMA increases arterial stiffness and decreases cerebral blood flow in humans. Stroke. 2006;37: 2024–9.
36. Czarnecka A, Milewski K, Zielińska M. Asymmetric dimethylarginine and hepatic encephalopathy: cause, effect or association? Neurochem Res. 2017;42:750–61.

37. Czarnecka A, Aleksandrowicz M, Jasiński K, Jaźwiec R, Kalita K, Hilgier W, et al. Cerebrovascular reactivity and cerebral perfusion of rats with acute liver failure: role of L-glutamine and asymmetric dimethylarginine in L-arginine-induced response. J. Neurochem. 2018;147:692–704.
38. Behrouzifar S, Vakili A, Bandegi AR, Kokhaei P. Neuroprotective nature of adipokine resistin in the early stages of focal cerebral ischemia in a stroke mouse model. Neurochem. Int. 2018;114:99–107.
39. Pei Z, Fung PC, Cheung RT. Melatonin reduces nitric oxide level during ischemia but not blood-brain barrier breakdown during reperfusion in a rat middle cerebral artery occlusion stroke model. J. Pineal Res. 2003;34:110–8.
40. Hayan D, Rodionov RN, Cynthia L, Cooke JP, Erland A, Teodoro B, et al. Overexpression of dimethylarginine dimethylaminohydrolase inhibits asymmetric dimethylarginine-induced endothelial dysfunction in the cerebral circulation. Stroke. 2008;39:180–4.
41. Murphy RB, Tommasi S, Lewis BC, Mangoni AA. Inhibitors of the hydrolytic enzyme dimethylarginine dimethylaminohydrolase (DDAH): discovery, synthesis and development. Molecules. 2016;21:615.
42. Böger RH. L-arginine improves vascular function by overcoming the deleterious effects of ADMA, a novel cardiovascular risk factor. Altern. Med. Rev. Altern. Med. Rev. 2005;10:14.
43. Jabecka A, Ast J, Bogdaski P, Drozdowski M, Pawlak-Lemaska K, Cielewicz AR, et al. Oral L-arginine supplementation in patients with mild arterial hypertension and its effect on plasma level of asymmetric dimethylarginine, L-citruline, L-arginine and antioxidant status. Eur. Rev. Med. Pharmacol. Sci. 2012;16: 1665–74.
44. Jiang, X, Andjelkovic, AV, Zhu, L, Yang, T, Bennett, MVL, Chen, J et al. Blood-brain barrier dysfunction and recovery after ischemic stroke. Prog. Neurobiol. 2018;163–4:144–71.
45. Prakash R, Carmichael ST. Blood-brain barrier breakdown and neovascularization processes after stroke and traumatic brain injury. Curr. Opin. Neurol. 2015;28:556–64.
46. Campisi M, Shin Y, Osaki T, Hajal C, Chiono V, Kamm RD. 3D self-organized microvascular model of the human blood-brain barrier with endothelial cells, pericytes and astrocytes. Biomaterials. 2018;180:117.
47. Gao W, Li F, Liu L, Xu X, Zhang B, Wu Y, et al. Endothelial colony-forming cell-derived exosomes restore blood-brain barrier continuity in mice subjected to traumatic brain injury. Exp. Neurol. 2018;307:99–108.
48. Panahpour, H, Farhoudi, M, Omidi, Y & Mahmoudi, J. An in vivo assessment of blood-brain barrier disruption in a rat model of ischemic stroke. J Vis Exp. 2018;133:57156.
49. Chen FQ, Li Q, Pan CS, Liu YY, Yan L, Sun K, et al. Kudiezi Injection(®) alleviates blood-brain barrier disruption after ischemia-reperfusion in rats. Microcirculation. 2016;23:426–37.
50. Abdullahi W, Tripathi D, Ronaldson P. Blood-brain barrier dysfunction in ischemic stroke: targeting tight junctions and transporters for vascular protection. Am. J. Physiol. Cell Physiol. 2018;315:C343–C356.
51. Ping Z, Xinli H, Xin X, Yingjie C, Bache RJ. Dimethylarginine dimethylaminohydrolase 1 modulates endothelial cell growth through nitric oxide and Akt. Arterioscler. Thromb. Vasc. Biol. 2011;31:890.
52. Choi S, Singh I, Singh A, Khan M, Won J. Asymmetric dimethylarginine exacerbates cognitive dysfunction associated with cerebrovascular pathology. FASEB J. 2020;34:6808–23.
53. Chen Y, Xu X, Sheng M, Zheng Z, Gu Q. Effects of asymmetric dimethylarginine on bovine retinal capillary endothelial cell proliferation, reactive oxygen species production, permeability, intercellular adhesion molecule-1, and occludin expression. Mol. Vis. 2011;17:332–40.